

A new approach to the investigation of load interaction effects and its application in residual fatigue life prediction

Zhaochun Peng, Hong-Zhong Huang, Hai-Kun Wang, Shun-Peng Zhu and Zhiqiang Lv

Abstract

Fatigue damage under variable amplitude loading is related to load histories, such as load sequences and load interactions. Many nonlinear damage models have been developed to present load sequences, but load interactions are often ignored. This paper provides a new approach to present load interaction effects for nonlinear damage accumulation. It is assumed that the ratio of two consecutive stress levels is used to describe the phenomenon on damage evolution. By introducing the approach to a nonlinear fatigue model without load interactions, a modified model is developed to predict the residual fatigue life under variable amplitude loading. Experimental data from three metallic materials and welded joints in the literature are employed to verify the effectiveness of the proposed method under two-level loading. The result shows that the modified model predicts more satisfactory estimations than the primary model and Miner rule. Furthermore, the proposed method is calibrated and validated by the case of multilevel loading. It is found that the modified model shows a good estimation and its damage curve presents a typical nonlinear behavior of damage growth. It is also convenient to calculate the residual fatigue life by the Wöhler curve.

Keywords

Fatigue, nonlinear damage accumulation, load interaction effects, variable amplitude loading, life prediction

Introduction

In engineering applications, many mechanical components and structures are generally subjected to complex cyclic loads with varying amplitudes. Fatigue is one of main failure modes for these components or structures during the service operation and it has been estimated to make up approximately 90% of metallic failures (Schijve, 2003; Schütz, 1996). As the fatigue loading proceeds,

Institute of Reliability Engineering, University of Electronic Science and Technology of China, Chengdu, Sichuan, China

Corresponding author:

Hong-Zhong Huang, Institute of Reliability Engineering, University of Electronic Science and Technology of China, Chengdu, Sichuan 611731, China.

Email: hzhuang@uestc.edu.cn

fatigue damage in materials or structures increases progressively in a cumulative manner, which may cause undesirable accidents and economic loss. Therefore, the fatigue life prediction is crucial to structural design, safe use, and reliability assessment. Due to the complex nature and importance of fatigue damage, assessing the damage evolution behavior is always a critical and complex subject (Cui, 2002; Yang and Fatemi, 1998). It is essential to present fatigue damage mechanisms significantly and contribute to the increasing precision of life prediction.

The current fatigue test data regarding stress–life or strain–life relation are easily accessible under constant amplitude loading (CAL). Assessing the residual life under variable amplitude loading (VAL) often relies on these available CAL data. Recently, many researchers have devoted their efforts to variable amplitude fatigue analyses and developed various life fraction models. Ghammouri et al. (2011) presented a plastic strain-controlled damage model in accordance with the evolution law of the principal crack to predict the residual life of Oxygen-Free High Thermal Conductivity (OFHC) copper. Huffman and Beckman (2013) used a phenomenological technique to establish a reversal-by-reversal cumulative damage rule for predicting the strain life under VAL. Kwofie and Rahbar (2013) proposed a fatigue driving stress model based on the S–N curve approach, and the residual life fraction was predicted by determining the same driving stress as the previous loads. Aid et al. (2011) put forward a damaged stress model on the grounds of the damage stress concept connected to the Wöhler curve, and then extended the model by using strain energy approaches (Djebli et al., 2013). In contrast, the most popular used theory in engineering designs is the Palmgren–Miner rule (Miner, 1945), commonly referred to as linear damage rule (LDR) or Miner rule, because of its conceptual simplicity, robustness, and easy implementation. This rule hypothesizes that the cumulative damage follows a simple linear trend. Mathematically, Miner rule is written as

$$D = \sum_{i=1}^k \frac{n_i}{N_{fi}} \quad (1)$$

where n_i is the number of loading cycles at a given stress level σ_i , N_{fi} is the fatigue life at σ_i under CAL, and D is the cumulative damage for a k -level block loading. The model defines fatigue damage as a life fraction n_i/N_{fi} for each applied stress level. Fatigue fracture of materials or components is assumed to occur when the sum of the life fractions reaches the critical damage, i.e. unity.

However, in the case of VAL, load histories (such as load sequences and load interactions) show a significant influence on fatigue damage evolution. Since Miner rule is load-level independent and fails to account for these load effects, it often leads to nonconservative predictions for high–low (H–L) loading and to conservative predictions for low–high (L–H) loading. Another limitation is that it is invalid when the applied loads are below the fatigue limit of the material. Due to its empirical nature and intrinsic insufficiencies, experimentally Miner rule is found to be inaccurate or yields larger prediction deviations (Böhm et al., 2014; Djebli et al., 2013; Zhu et al., 2011; Zuo et al., 2015). Several researchers further extend this basic rule, but the linear hypothesis and basic weaknesses remain in various extensions, and the results are still found to be unsatisfactory (Fatemi and Yang, 1998).

In order to alleviate the shortcomings associated with LDR, researchers have resorted to the nonlinear hypothesis that fatigue damage increases nonlinearly and damage rate is load dependent, which can present load sequence effects (Taheri et al., 2013). To date, many nonlinear life prediction models have been developed in accordance with various techniques. In general, they can be classified into three groups, i.e. phenomenological theories (Devulder et al., 2010; Huffman and Beckman, 2013; Pavlou, 2002; Yuan et al., 2015), continuum damage mechanics (CDM) (Ayoub et al., 2011;

Chaboche and Lesne, 1998; Tikri et al., 2014; Van Do et al., 2015; Yuan et al., 2013), and fracture mechanics (FM) (Cui et al., 2011; Manson and Halford, 1981; McEvily et al., 2005). Although most of these modeling methods are superior to the Miner rule, life predictions under VAL sometimes show a significant deviation from the experimental data.

Owing to the complexity of load histories, variable loading fatigue damage becomes much more intractable. Many researchers have reported that the load interaction effect is an important factor for the increased prediction accuracy. Among them, Corten and Dolan (1956) proposed the Corten–Dolan model according to the modified S–N curve, in which the load interaction effect was described as the ratio of different stress levels. Freudenthal and Heller (1959) also used a similar modification to present load interactions in the form of load ratio between stress levels. Morrow (1986) put forward a load interaction damage model based on Miner rule, and the form of load ratio was used to describe the interaction effect. Carpinteri et al. (2003) developed a damage model for multi-axial fatigue life prediction, and a load ratio parameter was found to calculate fatigue damage. More recently, Gao et al. (2014) and Yuan et al. (2015) considered the minimum load ratio between stress levels as a load interaction parameter to modify the Manson–Halford model, providing a good life estimation. Lv et al. (2015) also introduced a load ratio parameter to a fatigue damage model and obtained more exact predictions. In this regard, residual fatigue life under VAL can be dominated by the load interaction effect, and a load ratio parameter between stress levels is adequate to present this effect.

Although many efforts have been devoted to the knowledge of load interaction effects, the physical mechanisms responsible for the effects are still not clear. Some studies related under VAL can be utilized to explain the phenomenon. Morrow (1986) confirmed that micro-cracks were easily formed by large strains, and the subsequent small cycles would lead to the acceleration of crack propagation as a result of a premature failure. Skorupa (Skorupa, 1998, 1999) reported that the evolution behavior of crack growth under VAL differed from that under CAL. Shenoy et al. (2010) suggested that the crack growth for metallic materials was retarded when undergoing increasing fatigue loading, while accelerated for decreasing loading. Fatigue life under H–L loading was shorter than that under L–H loading, as presented by Fatemi and Yang (1998) and Liakat and Khonsari (2014). Freudenthal and Heller (1959) and Aghoury and Galal (2013) pointed out that the damaging effect was related to the magnitude of applied stress amplitudes. These studies suggest that the increase or decrease of applied stress amplitudes will cause the variation of damage evolution. The previous cycles at some stress level can affect the damage evolution by the subsequent cycles at a different stress level. The damage rate should be associated with the magnitude of applied loads.

The aim of this paper is to investigate the evolution behavior of the fatigue damage induced by the load interactions under VAL. Based on the nonlinear damage accumulation, a new approach considering the load interaction effect is proposed. It assumes that the ratio of two consecutive stress levels is used to characterize the effect on damage evolution. Then, the method is introduced to a nonlinear damage model without load interactions, and a modified model is thus formulated to predict residual fatigue life. The experimental data from a series of two-level loading and multilevel loading are used to verify the effectiveness of the proposed method.

Formulation of a new approach to present load interaction effects

Many studies have highlighted that most of metallic materials commonly present a nonlinear damage behavior with load-level dependence (Pereira et al., 2008). It often generates a higher damage rate when the material is subjected to a higher stress level. In general, the damage variable

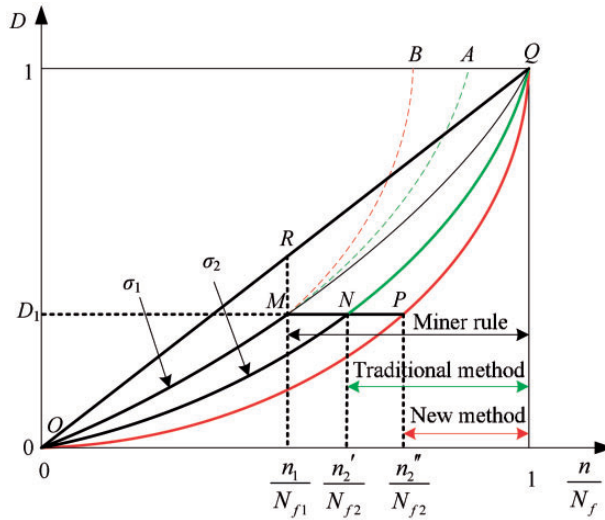


Figure 1. Schematic representation of the damage evolution under two-level H–L fatigue loading.

is related to the applied load and the consumed life fraction. In the case of CAL, it can be expressed by a general function as follows

$$D = f(\sigma, n/N_f) \tag{2}$$

For a two-level H–L fatigue loading, the metallic specimen is applied at a higher stress amplitude σ_1 for n_1 cycles firstly, then at a lower stress amplitude σ_2 for n_2 cycles up to the failure. Figure 1 shows a schematic representation of the damage evolution under such loading condition. The non-linear damage evolution curves for σ_1 and σ_2 under CAL are OMQ and ONQ, respectively.

Due to the equivalent characteristic of damage introduced by Richart and Newmark (1948), equal damage rule is often used to predict the residual life under VAL. In order to present the damaged degree of the material, a concept of fatigue damage state (FDS) is introduced and characterized by a notation with respect to the applied stress amplitude, the number of loading cycles, and the cumulative damage, shown as

$$FDS : (\sigma, n, f(\sigma, n/N_f)) \tag{3}$$

Equation (3) captures the instantaneous damage behavior and the current fatigue loading state. From Figure 1, the first stress amplitude σ_1 for n_1 cycles will produce the damage D_1 , which is equal to that caused by the second stress amplitude σ_2 for n'_2 cycles. Conventionally, the damage accumulation evolution follows the curve OMNQ, and the equal FDS takes the form

$$FDS_1 : (\sigma_1, n_1, f(\sigma_1, n_1/N_{f1})) = FDS_2 : (\sigma_2, n'_2, f(\sigma_2, n'_2/N_{f2})) \tag{4}$$

Thus, a prediction of residual life fraction n_2/N_{f2} at σ_2 can be determined by

$$f(\sigma_1, n_1/N_{f1}) = f(\sigma_2, 1 - n_2/N_{f2}) \tag{5}$$

Using equation (4), a two-level variable fatigue loading will be degenerated into an equal constant amplitude fatigue loading at the subsequent stress, which still maintains its original damage evolution ONQ. However, Xie et al. (1994) and Xie (1995) performed a series of two-level fatigue tests and found that the conventional equal FDS did not exist for different stress levels. It suggests that the significance of equations (4) and (5) is insufficient and it may lead to large prediction errors.

For the case of two-level H–L loading in Figure 1, due to the load interaction effects, the prior fatigue loading at the first stress σ_1 can affect the damage evolution at the second stress σ_2 . The subsequent cycles at σ_2 tend to accelerate the damage accumulation as a result of a shorter fatigue life. Thus, the damage evolution at σ_2 will deviate from its primary law (NQ or MA after translation, see Figure 1). Assuming that the damage law at σ_2 follows the curve MB, a complete CAL damage evolution at σ_2 becomes the curve OPQ (the damage function is assumed as $D = f'(\sigma_2, n/N_{f2})$) with a translation of MB. In addition, the difference between the damage curves NQ and PQ depends on the magnitude of applied stresses. According to the equal damage rule, the cumulative damage D_1 is equivalent to that caused by σ_2 at a life fraction of n_2''/N_{f2} (see Figure 1). Consequently, a new fatigue damage evolution accounting for load interaction effects follows the curve OMPQ. Accordingly, the equal FDS for these two stress amplitudes takes the form

$$FDS_1 : (\sigma_1, n_1, f(\sigma_1, n_1/N_{f1})) = FDS_2' : (\sigma_2, n_2'', f'(\sigma_2, n_2''/N_{f2})) \quad (6)$$

In order to present the damage function $f'(\sigma_2, n/N_{f2})$, the basic conditions should be satisfied as follows

$$0 \leq f'(\sigma_2, n/N_{f2}) \leq 1 \quad (7)$$

$$f'(\sigma_2, 0) = 0 \quad (8)$$

$$f'(\sigma_2, 1) = 1 \quad (9)$$

$$f'(\sigma_2, n/N_{f2}) < f(\sigma_2, n/N_{f2}) \quad (10)$$

For two-level L–H loading, equation (10) should be written as

$$f'(\sigma_2, n/N_{f2}) > f(\sigma_2, n/N_{f2}) \quad (11)$$

Mathematically, to meet the above-mentioned conditions, a power law is suitable to present the relationship between $f'(\sigma_2, n/N_{f2})$ and $f(\sigma_2, n/N_{f2})$. Besides, the damage evolution (D vs. n/N_f) under CAL can be expressed as some power function, such as Marco–Starkey's model or Manson's model (Fatemi and Yang, 1998). The damage function $f'(\sigma_2, n/N_{f2})$ can be obtained by $f(\sigma_2, n/N_{f2})$ through the change of power exponent. Hence, a power law is relatively reasonable to present this relation, that is

$$f'(\sigma_2, n/N_{f2}) = [f(\sigma_2, n/N_{f2})]^{\omega_{1,2}} \quad (12)$$

where $\omega_{1,2}$ is interpreted as an interaction factor to present the load interaction effect between σ_1 and σ_2 .

Using equation (6), the two-level fatigue loading is also degenerated into an equal CAL at the subsequent stress. In this way, a three-level loading is firstly degenerated into an equal CAL at the

second stress, and then another one at the third stress. Thus, the interaction factor is directly dependent on the two consecutive stress levels. The value of $\omega_{1,2}$ should be greater than 1 for H–L loading, while lower than 1 for L–H loading. If the applied stresses are equal, load interaction effects should not exist, i.e. $\omega_{1,2} = 1$. Previous researches (Gao et al., 2014; Lv et al., 2015; Yuan et al., 2015) have also shown that the form of load ratio can be used to describe load interaction effects, and a large difference between stress levels leads to a stronger interaction effect. Therefore, the parameter $\omega_{1,2}$ can be assumed as $\omega_{1,2} = \sigma_1/\sigma_2$ and equation (12) is rewritten as

$$f(\sigma_2, n/N_{f2}) = [f(\sigma_2, n/N_{f2})]^{\sigma_1/\sigma_2} \tag{13}$$

A new prediction of n_2/N_{f2} at σ_2 can be determined by

$$f(\sigma_1, n_1/N_{f1}) = [f(\sigma_2, 1 - n_2/N_{f2})]^{\sigma_1/\sigma_2} \tag{14}$$

In the same way, for a three-level loading, the residual life fraction n_3/N_{f3} at the third stress level σ_3 can be derived from

$$[f(\sigma_2, (n_2'' + n_2)/N_{f2})]^{\sigma_1/\sigma_2} = [f(\sigma_3, 1 - n_3/N_{f3})]^{\sigma_2/\sigma_3} \tag{15}$$

For i -level ($i \geq 3$) fatigue loading, the following symbols are defined for the purpose of simplicity

$$\tilde{n}_{i-1}/N_{f(i-1)} = (n_{i-1}'' + n_{i-1})/N_{f(i-1)} \tag{16}$$

$$\omega_{i-1,i} = \sigma_{i-1}/\sigma_i \tag{17}$$

Similarly, the residual life fraction n_i/N_{fi} at the last stress level σ_i can be obtained as

$$[f(\sigma_{i-1}, \tilde{n}_{i-1}/N_{f(i-1)})]^{\omega_{i-2,i-1}} = [f(\sigma_i, 1 - n_i/N_{fi})]^{\omega_{i-1,i}} \tag{18}$$

A modified nonlinear model with the use of the proposed method

In general, the fatigue failure is considered as an irreversible process of physical properties degradation in materials. The definition of damage variable is particularly important to present the damage evolution. Many researchers have developed a series of damage models with different state variables of materials, such as modulus of elasticity, fatigue limit, tensile strength, stiffness, static toughness, etc. Among them, Ye and Wang (2001) developed a nonlinear damage model (referred to as Ye’s model) based on the static toughness exhaustion in materials, while also demonstrating its applicability by a series of uniaxial fatigue experimental data within both low-cycle and high-cycle fatigue regimes. The model is adequate to characterize the fatigue damage process because of its simplicity, clear physical connotation, and sensitivity. The cumulative damage formula is expressed as

$$D = -\frac{D_{N_f-1}}{\ln N_f} \ln\left(1 - \frac{n}{N_f}\right) \tag{19}$$

where D_{N_f-1} is the critical damage after $N_f - 1$ cycles at a certain stress level. Ye et al. (1999) suggested that the parameter of D_{N_f-1} was approximately equal to unity in theory. Liakat and

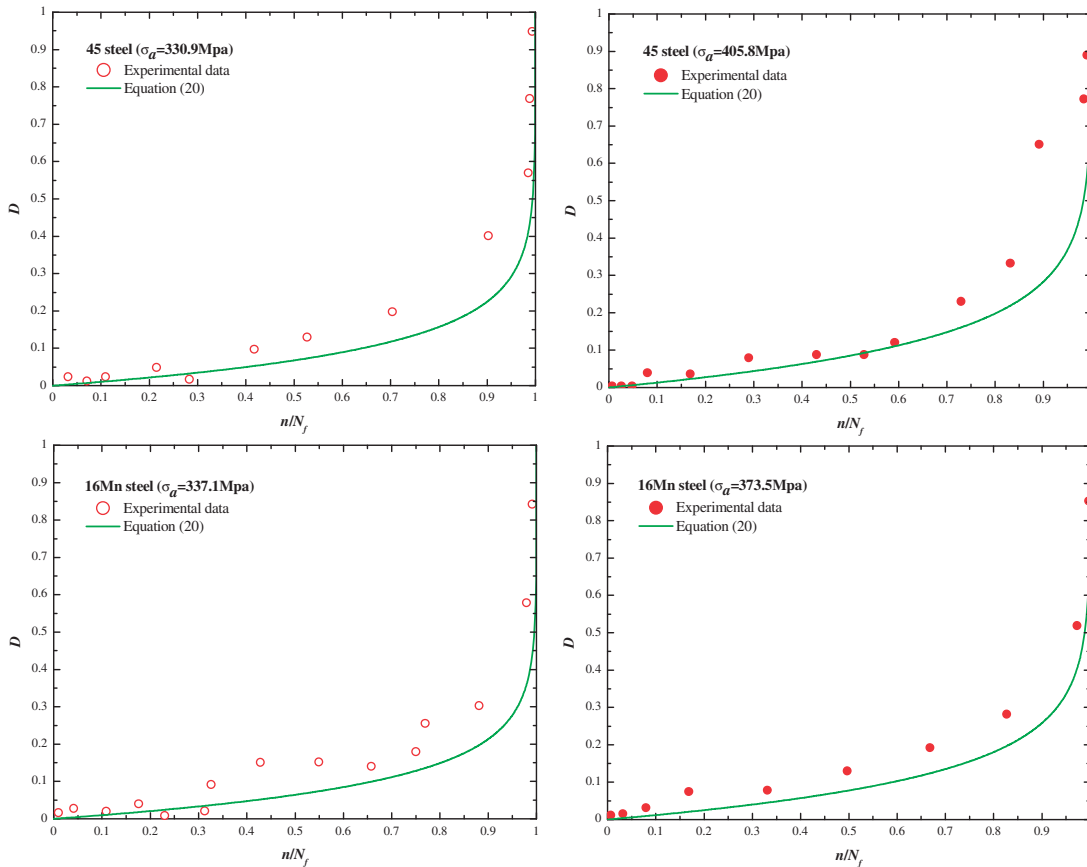


Figure 2. Comparisons between the damage evolution curves using equation (20) and experimental results for 45 steel and 16Mn steel under CAL.

Khonsari (2014) subsequently conducted a series of monotonic static tests and also found that the parameter was very close to unity, i.e. $D_{N_f-1} \approx 1$. Thus, equation (19) can be simplified as

$$D \approx -\frac{\ln(1 - \frac{n}{N_f})}{\ln N_f} \quad (20)$$

For this nonlinear damage formula, the experimental data of 45 steel and 16Mn steel (Shang and Yao, 1999) are employed to present the significance. Plots of the damage variable D versus the consumed life fraction n/N_f for constant amplitude tests are shown in Figure 2. It can be observed that the theoretical damage evolution curves show a good correlation with the experimental data.

For the case of two-level loading, according to equations (5) and (20), the prediction of residual life fraction at the second stress level can be obtained as

$$\frac{n_2}{N_{f2}} = \left(1 - \frac{n_1}{N_{f1}}\right)^{\frac{\ln N_{f2}}{\ln N_{f1}}} \quad (21)$$

For H–L loading sequence, i.e. $\sigma_1 > \sigma_2$, $N_{f1} < N_{f2}$, the sum of life fractions is

$$\frac{n_1}{N_{f1}} + \frac{n_2}{N_{f2}} = \frac{n_1}{N_{f1}} + \left(1 - \frac{n_1}{N_{f1}}\right)^{\frac{\ln N_{f2}}{\ln N_{f1}}} < 1 \tag{22}$$

For L–H loading sequence, i.e. $\sigma_1 < \sigma_2$, $N_{f1} > N_{f2}$, it is

$$\frac{n_1}{N_{f1}} + \frac{n_2}{N_{f2}} = \frac{n_1}{N_{f1}} + \left(1 - \frac{n_1}{N_{f1}}\right)^{\frac{\ln N_{f2}}{\ln N_{f1}}} > 1 \tag{23}$$

The results are consistent with many experimental evidences, showing that the nonlinear damage model of equation (20) is capable of predicting the load sequence effect responsible for the variable fatigue loading.

In the same way, for multilevel loading condition, it is easy to obtain the residual life fraction at the last stress level σ_i , that is

$$\frac{n_i}{N_{fi}} = \left(1 - \left(\frac{n'_{i-1}}{N_{f(i-1)}} + \frac{n_{i-1}}{N_{f(i-1)}}\right)\right)^{\frac{\ln N_{fi}}{\ln N_{f(i-1)}}} \tag{24}$$

where $n'_{i-1}/N_{f(i-1)}$ is the equivalent life fraction at the $(i - 1)$ th loading level.

However, equation (20) does not lay enough emphasis on the effect of load interactions between stress levels (Yang et al., 2003), and the damage evolution can be dominated by this effect during the entire fatigue process. Then, a modification with the use of the proposed method, as presented in the second section, is developed to predict the residual fatigue life.

Combining equations (14) and (20), the predicted residual life fraction at σ_2 under two-level loading is

$$\left(\frac{n_2}{N_{f2}}\right)_{mp} = \left(\frac{1}{N_{f2}}\right) \left[\frac{-\ln\left(1 - \frac{n_1}{N_{f1}}\right)}{\ln N_{f1}} \right]^{\frac{\sigma_2}{\sigma_1}} \tag{25}$$

where the subscript *mp* denotes the prediction of the modified model. Suppose that the applied loads remain the same, i.e. $\sigma_1 = \sigma_2$, $N_{f1} = N_{f2}$, equation (25) is reduced as the Miner’s LDR

$$\frac{n_2}{N_{f2}} = 1 - \frac{n_1}{N_{f1}} \tag{26}$$

For the case of three-level loading, substituting equation (20) into equation (15), the residual life fraction at the third stress level σ_3 can be obtained by using an iterative procedure, that is

$$\left(\frac{n_3}{N_{f3}}\right)_{mp} = \left(\frac{1}{N_{f3}}\right) \left[\frac{-\ln\left(\left(\frac{n_2}{N_{f2}}\right)_{mp} - \frac{n_2}{N_{f2}}\right)}{\ln N_{f2}} \right]^{\frac{\sigma_1 \times \sigma_3}{\sigma_2 \times \sigma_2}} \tag{27}$$

It is noted that equation (27) can be generalized to the multilevel loading. The residual life fraction at the last loading level is derived as

$$\left(\frac{n_i}{N_{fi}}\right)_{mp} = \left(\frac{1}{N_{fi}}\right) \left[\frac{-\ln\left(\left(\frac{n_{i-1}}{N_{f(i-1)}}\right)_{mp} - \frac{n_{i-1}}{N_{f(i-1)}}\right)}{\ln N_{f(i-1)}} \right]^{\frac{\sigma_{i-2} \times \sigma_i}{\sigma_{i-1} \times \sigma_{i-1}}} \quad (28)$$

It can be seen that equations (25), (27), and (28) depend on the parameters of the applied loads and their fatigue lives, and these parameters can be easily obtained by the stress–life relation, i.e. Wöhler curve. These modifications are also appropriate to the increasing and decreasing fatigue loadings.

Experiments and discussions

In this section, the experimental data from two-level loading and multilevel loading are employed to demonstrate the descriptive ability of the proposed method. In order to assess the validity of predicted results, the relative error of prediction (REP) is introduced to present the difference between the experimental and predicted results, which is defined as

$$\text{REP} = \left| \frac{(n/N_f)_{\text{experimental}} - (n/N_f)_{\text{predicted}}}{(n/N_f)_{\text{experimental}}} \right| \times 100 \quad (29)$$

where $(n/N_f)_{\text{experimental}}$ and $(n/N_f)_{\text{predicted}}$ are the experimental and predicted life fraction, respectively.

Two-level loading condition

Case 1: 45 steel. The material studied here is the normalized 45 steel (Shang and Yao, 1999). The uniaxial rotating bending tests were conducted under the stress-controlled and fully reversed loading condition (the stress ratio $R = -1$) with the H–L and L–H loading patterns. The ultimate tensile strength and the fatigue limit of the material are $\sigma_b = 598.2$ MPa and $\sigma_{-1} = 262.8$ MPa, respectively. The higher and lower loading stress amplitudes are $\sigma_a = 331.5$ MPa and $\sigma_a = 284.4$ MPa, and the H–L and L–H load spectrums are 331.5 – 284.4 MPa and 284.4–331.5 MPa, respectively. Table 1 lists the loading condition, experimental data, and predicted results obtained by Miner rule, Ye's model, and the modified model. Figures 3 and 4 also illustrate the predictions using these three models under H–L and L–H loading sequences, respectively.

Case 2: Aluminium alloy Al-2024. The material used in this case is aluminium alloy Al-2024 (Aid et al., 2011; Pavlou, 2002), which is widely used for aerospace applications. The uniaxial fatigue tests were performed under complete reverse bending loading at the frequency of 25 Hz. The stress ratio is held constant ($R = -1$), and the mean stress is zero. Two loading stress amplitudes are considered, i.e. $\sigma_a = 200$ MPa and $\sigma_a = 150$ MPa. The load spectrums under H–L and L–H loading sequence are 200 – 150 MPa and 150–200 MPa, respectively. Table 2 also lists the loading condition, experimental data, and the corresponding predicted results calculated by Miner rule,

Table 1. Experimental data and the predicted results obtained by Miner rule, Ye’s model, and the modified model for 45 steel.

Loading condition	Experimental data				Predicted results using different models					
					Miner rule		Ye’s model		Modified model	
	n_1	n_1/N_{f1}	n_2	n_2/N_{f2}	n_2/N_{f2}	REP (%)	n_2/N_{f2}	REP (%)	n_2/N_{f2}	REP (%)
H–L $\sigma_1 = 331.5$ MPa $\sigma_2 = 284.4$ MPa	500	0.0100	423,700	0.8474	0.9900	16.83	0.9879	16.58	0.9677	14.20
	12,500	0.2500	250,400	0.5008	0.7500	49.76	0.7055	40.87	0.5576	11.34
	25,000	0.5000	168,300	0.3366	0.5000	48.54	0.4314	28.16	0.2888	14.20
	37,500	0.7500	64,500	0.1290	0.2500	93.80	0.1861	44.26	0.1053	18.37
L–H $\sigma_1 = 284.4$ MPa $\sigma_2 = 331.5$ MPa	125,000	0.2500	37,900	0.7580	0.7500	1.06	0.7888	4.06	0.8816	16.31
	250,000	0.5000	38,900	0.7780	0.5000	35.73	0.5647	27.42	0.7039	9.52
	375,000	0.7500	43,400	0.8680	0.2500	71.20	0.3188	63.27	0.4549	47.59

Note: REP: relative error of prediction.

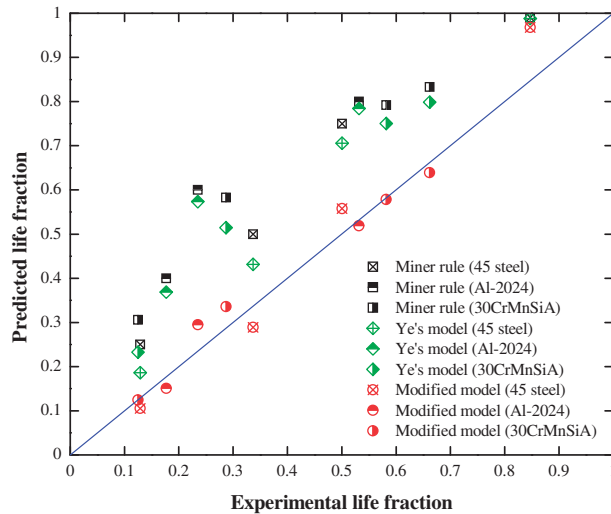


Figure 3. Comparison between the experimental and predicted results for 45 steel, Al-2024, and 30CrMnSiA under H–L loading sequence.

Ye’s model, and the modified model. A graph comparison of these models for both H–L and L–H loading sequences is shown in Figures 3 and 4, respectively.

Case 3: 30CrMnSiA. The material of 30CrMnSiA is used in this case (Fang et al., 2006). The tests were carried out under uniaxial two-level stress loading for both H–L and L–H loading sequences. The mean stress under different loading sequences is held constant ($\sigma_m = 250$ MPa), and the maximum stresses of the applied loads are $\sigma_{max} = 836$ MPa and $\sigma_{max} = 732$ MPa. The higher and lower stress amplitudes are $\sigma_a = 586$ MPa and $\sigma_a = 482$ MPa, and the corresponding stress ratios are

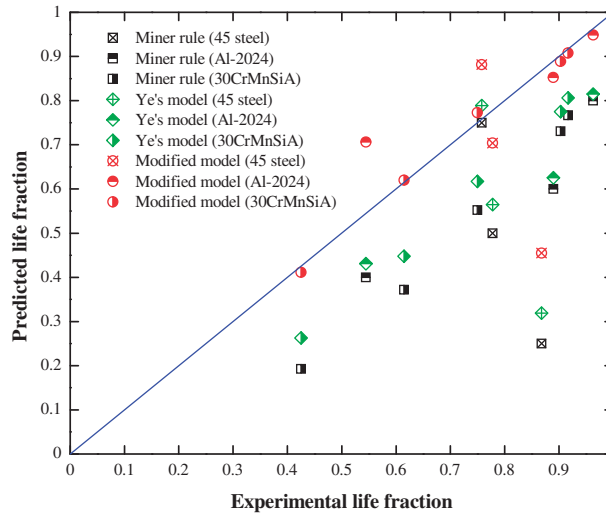


Figure 4. Comparison between the experimental and predicted results for 45 steel, Al-2024, and 30CrMnSiA under L-H loading sequence.

Table 2. Experimental data and the predicted results obtained by Miner rule, Ye’s model, and the modified model for aluminium alloy Al-2024.

Loading condition	Predicted results using different models									
	Experimental data				Miner rule		Ye’s model		Modified model	
	n_1	n_1/N_{f1}	n_2	n_2/N_{f2}	n_2/N_{f2}	REP (%)	n_2/N_{f2}	REP (%)	n_2/N_{f2}	REP (%)
H-L $\sigma_1 = 200$ MPa $\sigma_2 = 150$ MPa	30,000	0.2000	228,700	0.5319	0.8000	50.40	0.7844	47.47	0.5186	2.50
	60,000	0.4000	101,050	0.2350	0.6000	155.32	0.5735	144.04	0.2947	25.40
	90,000	0.6000	76,050	0.1769	0.4000	126.12	0.3689	108.54	0.1505	14.92
L-H $\sigma_1 = 150$ MPa $\sigma_2 = 200$ MPa	86,000	0.2000	144,500	0.9633	0.8000	16.95	0.8146	15.44	0.9484	1.55
	172,000	0.4000	133,500	0.8900	0.6000	32.58	0.6254	29.73	0.8524	4.22
	258,000	0.6000	81,700	0.5447	0.4000	26.57	0.4309	20.89	0.7061	29.63

Note: REP: relative error of prediction.

$R = -0.402$ and $R = -0.317$, respectively. The H-L and L-H load spectrums are 586 – 482 MPa and 482–586 MPa, respectively. Test parameters and the predicted results are shown in Table 3. A comparison between the experimental results and models predictions under H-L and L-H loading sequences is also depicted in Figures 3 and 4, respectively.

According to the present results, as summarized in Tables 1 to 3, it is found that the modified model presents a good correlation between the experimental and predicted results. The modified model and Ye’s model predict $\sum (n_i/N_{fi}) < 1$ for H-L loading sequence and $\sum (n_i/N_{fi}) > 1$ for L-H loading sequence, while Miner rule always gives $\sum (n_i/N_{fi}) = 1$ whatever the loading sequence. This phenomenon is consistent with many experimental evidences in the literature. It suggests that fatigue

Table 3. Experimental data and the predicted results obtained by Miner rule, Ye's model, and the modified model for 30CrMnSiA.

Loading condition	Experimental data				Predicted results using different models					
					Miner rule		Ye's model		Modified model	
	n_1	n_1/N_{f1}	n_2	n_2/N_{f2}	n_2/N_{f2}	REP (%)	n_2/N_{f2}	REP (%)	n_2/N_{f2}	REP (%)
H-L $\sigma_1 = 586$ MPa $\sigma_2 = 482$ MPa	1200	0.1670	36,911	0.6620	0.8330	25.83	0.7986	20.63	0.6389	3.49
	1800	0.2080	32,450	0.5820	0.7920	36.08	0.7505	28.95	0.5784	0.62
	3000	0.4170	16,002	0.2870	0.5830	103.14	0.5147	79.34	0.3357	16.97
	5000	0.6940	6969	0.1250	0.3060	144.80	0.2328	86.24	0.1245	0.40
L-H $\sigma_1 = 482$ MPa $\sigma_2 = 586$ MPa	13,000	0.2330	6602	0.9170	0.7670	16.36	0.8061	12.09	0.9079	0.99
	15,000	0.2690	6501	0.9030	0.7310	19.05	0.7752	14.15	0.8884	1.62
	25,000	0.4480	5400	0.7500	0.5520	26.40	0.6171	17.72	0.7729	3.05
	35,000	0.6280	4428	0.6150	0.3720	39.51	0.4478	27.19	0.6197	0.76
	45,000	0.8070	3254	0.4250	0.1930	54.59	0.2627	38.19	0.4113	3.22

Note: REP: relative error of prediction.

damage evolution is sensitive to the load sequence effect, and the modified model and Ye's model are capable of presenting this effect on damage accumulation. In addition, in Figures 3 and 4, it is clear that Ye's model gives better results than Miner rule; the predictions using the modification show lesser deviations with the experimental data and are more representative than those of other models. Among these three models, the Miner's LDR should be still dominantly used in engineering designs, because of its conceptual simplicity. However, this model does not take load histories information into account, resulting in a large deviation with the reality. Although Ye's model can present load sequences, the model predictions are found to be slightly better than those of the Miner rule. It may not be sufficient to present the damage evolution when only considering the nonlinear load sequence effects, because of the complex loading histories. Making use of the proposed method, the modified model is developed to incorporate the effects of load sequences and load interactions and thus generates greater prediction accuracies. Therefore, the proposed method presents a possible scenario to characterize load interaction effects between consecutive stress levels, and the modified model allows us to correctly predict the residual life for different loading configurations.

Case 4: Results from the welded joints. In order to further verify the effectiveness of the proposed method under two-level loading, the modified model is applied to assess the fatigue life of welded joints, which are widely used in many engineering designs. Results from two kinds of welded aluminum alloy joints (butt joint and fillet joint) of Electric Multiple Units (Tian et al., 2012) are used in this case. The uniaxial fatigue tests were performed on a PLG-200 high-frequency testing machine under four-point bending loading with the stress ratio $R = -1$ ($\sigma_m = 0$). The experimental data were obtained by various combinations of two-level stress loading for both H-L and L-H loading sequences. For butt joint tests, three applied stress amplitudes were considered, i.e. $\sigma_a = 104$ MPa, $\sigma_a = 89$ MPa, and $\sigma_a = 74$ MPa. Four combinations of the load spectrums are 104 – 74 MPa and 89 – 74 MPa for H-L loading, and 74–89 MPa and 74–104 MPa for L-H loading, respectively. For fillet joint tests, three loading stress amplitudes were applied, i.e. $\sigma_a = 93$ MPa, $\sigma_a = 83$ MPa,

and $\sigma_a = 73$ MPa. Four combinations of the load spectrums are 93 – 73 MPa and 83 – 73 MPa for H–L loading, and 73–83 MPa and 73–93 MPa for L–H loading, respectively.

In this case, Tian et al. (2012) also proposed a nonlinear damage model based on damage curve approaches, which is called the existing model and is briefly described as follows

$$D = \left(\frac{n}{N_f} \right)^{1 + \left(\log_2 \frac{\sigma}{\sigma_s} \right)^t} \quad (30)$$

where σ_s is the yield strength of the welded joint, and t denotes the influence degree of load sequences and is determined by the experimental data. For the case of two-level loading, using the equal damage rule, the residual life fraction at the second stress level is given as

$$\frac{n_2}{N_{f2}} = 1 - \left(\frac{n_1}{N_{f1}} \right)^{1 + \left(\log_2 \frac{\sigma_1}{\sigma_s} \right)^t} \quad (31)$$

The details of the loading condition, experimental data, and models predictions are summarized in Table 4. A comparison between the experimental and predicted life fractions at the second stress level for H–L and L–H loading sequences is also represented in Figure 5.

From Figure 5, it is clear that the modified model substantially shows a better prediction performance than Ye's model and Miner rule. In addition, Table 4 unfolds a clear comparison of REPs calculated by different damage models. It is observed that 75% of the predictions using the modified model are better than those of Ye's model and Miner rule; the modified model also yields lower prediction errors (seven out of eight REPs < 19%) than Ye's model (seven out of eight REPs < 32%) and Miner rule (seven out of eight REPs < 35%). It is also found that the sum of life fractions using the Miner rule is equal to 1, and other three models predict that the Miner's damage sums are less than 1 for H–L loading and greater than 1 for L–H loading. The results suggest that the damage evolution behavior under VAL shows a strong dependence of the load sequence effect. It is noteworthy that the existing model shows great advantage of prediction performance over other models, and all the REPs fall within 9%. The reason is most likely due to the fact that the existing model takes extra parameter σ_s into account and also correctly presents the load sequence effects on damage accumulation. However, the model does not provide the interpretation of the load interaction effect, which may be an important factor to govern the failure process during fatigue. On the other hand, the existing model is a modified version of Marco–Starkey's model (Miner, 1945), and the determination of the parameter t is difficult and complex, especially for multilevel loading conditions. Moreover, the modified model does not need to fit more necessary parameters, and life prediction can be easily obtained with the use of Wöhler curve.

Multilevel loading condition

The material of 41Cr4 (Zhu et al., 2011) is used to validate the proposed method under multilevel loading. The uniaxial cyclic bending tests were carried out under eight-level stress loading with decreasing loading sequence. The stress ratio was set to be $R = -1$, and the fatigue limit of the material is $\sigma_{-1} = 173.5$ MPa. A detailed overview of loading conditions, experimental data, and models predictions is shown in Table 5. It should be noted that the last two stress levels are below

Table 4. Experimental data and the predicted results obtained by Miner rule, Ye's model, existing model and the modified model for welded joints.

Loading condition	Experimental data		Predicted results using different models											
			Miner rule			Ye's model			Existing model			Modified model		
	$n_1/10^3$	$n_2/10^3$	n_2/N_f	n_2/N_f	REP (%)	n_2/N_f	REP (%)	n_2/N_f	REP (%)	n_2/N_f	REP (%)	n_2/N_f	REP (%)	
Butt joint under H-L loading														
$\sigma_1 = 104$ MPa	109.9	797.6	0.5179	0.8000	54.47	0.7862	51.81	0.5528	6.74	0.4581	11.55			
$\sigma_2 = 74$ MPa	176.1	1029.2	0.6683	0.8000	19.71	0.7927	18.61	0.6316	5.49	0.6283	5.99			
Butt joint under L-H loading														
$\sigma_1 = 74$ MPa	770.1	545.6	0.6196	0.5000	19.30	0.5138	17.08	0.6728	8.59	0.6971	12.51			
$\sigma_2 = 89$ MPa	770.1	418.9	0.7626	0.5000	34.43	0.5257	31.06	0.7500	1.65	0.8280	8.58			
Fillet joint under H-L loading														
$\sigma_1 = 93$ MPa	309.9	587.5	0.3800	0.5000	31.58	0.4768	25.47	0.3735	1.71	0.2469	35.03			
$\sigma_2 = 73$ MPa	476.1	681.1	0.4405	0.5001	13.53	0.4880	10.78	0.4282	2.79	0.3576	18.82			
Fillet joint under L-H loading														
$\sigma_1 = 73$ MPa	509.2	708.2	0.7437	0.6707	9.82	0.6799	8.58	0.7478	0.55	0.7894	6.15			
$\sigma_2 = 83$ MPa	773.0	426.4	0.6880	0.5000	27.33	0.5227	24.03	0.6421	6.67	0.7533	9.49			

Note: REP: relative error of prediction.

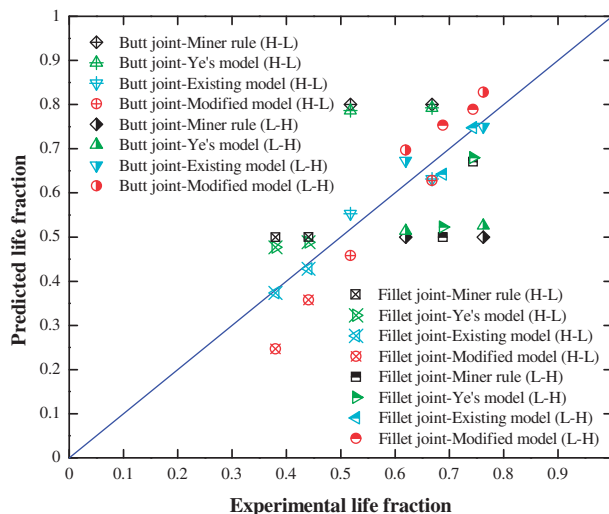


Figure 5. Comparison between the experimental and predicted life fractions for welded joints under H–L and L–H loading sequences.

Table 5. Experimental data and the predicted results obtained by Miner rule, Ye’s model, and the modified model for 41Cr4.

Loading condition		Experimental data		Predicted results using different models						
				Miner rule		Ye’s model		Modified model		
Stress level	Stress amplitude σ_i (MPa)	n_i	N_{fi}	n_i/N_{fi}	n_6/N_{f6}	$\sum(n_i/N_{fi})$	n_6/N_{f6}	$\sum(n_i/N_{fi})$	n_6/N_{f6}	$\sum(n_i/N_{fi})$
1	505	4	9.00×10^3	0.0004	–	0.0004	–	0.0004	–	0.0004
2	475	32	1.16×10^4	0.0028	–	0.0032	–	0.0032	–	0.0032
3	423	560	2.10×10^4	0.0267	–	0.0299	–	0.0299	–	0.0299
4	362	5440	4.70×10^4	0.1157	–	0.1456	–	0.1456	–	0.1456
5	287	40,000	1.55×10^5	0.2581	–	0.4037	–	0.4037	–	0.4037
6	212	184,000	8.70×10^5	0.2115	0.5963	1.0000	0.5348	0.9385	0.3935	0.7972
7	137	560,000	∞	0	–	1.0000	–	0.9385	–	0.7972
8	63	1,210,000	∞	0	–	1.0000	–	0.9385	–	0.7972

the fatigue limit and give no contribution to the cumulative fatigue damage for these three used models. Then, the sixth life fraction n_6/N_{f6} is chosen to compare the models prediction performances.

From Table 5, it shows that the prediction using the modified model is closer to the experimental life fraction at the sixth stress level than that of other models. For this decreasing fatigue loading, the modified model and Ye’s model again show the same trend in that $\sum(n_i/N_{fi}) < 1$,

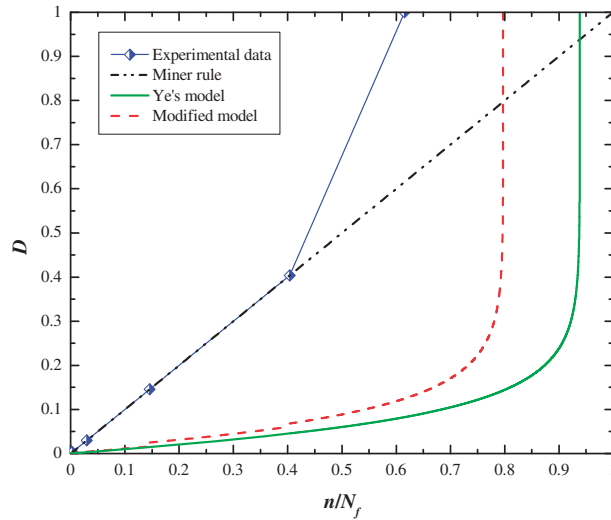


Figure 6. Plots of the damage evolution versus the consumed life fraction for Miner rule, Ye's model, and the modified model under decreasing loading condition.

while Miner rule yields $\sum (n_i/N_{fi}) = 1$. This once again suggests that the damage evolution under VAL is dominated by the load sequence effects. It should be anticipated that the modified model considers both load sequences and load interactions and thus gives more reasonable and representative prediction.

In this case, plots of the damage evolution versus the consumed life fraction for these three models are also illustrated in Figure 6. The damage evolution for the experimental data is calculated by the Miner's damage sums. During the entire fatigue life cycles, the damage curves calculated by the modified model and Ye's model present a concave form. It suggests that the cumulative damage remains low during the majority of the life fraction and then presents a sudden increase up to the final fracture; the damage accumulation is nonlinear. This observation agrees with the fatigue behaviors for most metallic materials.

The findings of the present study are verified under uniaxial VALs, it may be extended to the multiaxial loading with the use of multiaxial criterion. It is desirable to check the applicability of the proposed method for different materials and structures, especially for real structures in service under complex loading conditions (repeated block loading or random loading). Moreover, the damage evolution for variable fatigue loading often exhibits high complexities and involves various factors (such as mean stress, loading type, etc.). Therefore, further study on the fatigue evolution behavior and damage accumulation is also needed for accurate life assessments.

Conclusions

The paper attempts to present the evolution law of variable loading fatigue damage induced by the load interactions. Based on the comparison between the predicted results and experimental data in the literature, the main conclusions can be summarized as follows:

1. Based on the nonlinear damage accumulation, the fatigue damage evolution behavior under VAL is studied and a new approach to present the load interaction effect is proposed. The load ratio

- between two consecutive stress levels is employed to characterize the effect. It offers a good phenomenological understanding of fatigue damage evolution.
2. By introducing the approach to a nonlinear damage model, a modified model is formulated and verified using the experimental data (three metallic materials and welded joints) under two-level loading conditions. Comparing with the Miner rule and Ye's model, the modified model gives more satisfactory predictions and presents the capability of incorporating the effects of load sequences and load interactions. It is also convenient to predict the residual life with the use of Wöhler curve.
 3. The modified model is further calibrated and validated by the case of the material 41Cr4 under multilevel loading. According to the results obtained, the prediction using this modification is reasonable and representative, and the corresponding damage curve presents a typical nonlinear behavior of damage growth.

Declaration of Conflicting Interests

The author(s) declared no potential conflicts of interest with respect to the research, authorship, and/or publication of this article.

Funding

The author(s) disclosed receipt of the following financial support for the research, authorship, and/or publication of this article: The present research was supported by NSAF under Grant No. U1330130.

References

- Aid A, Amrouche A, Bouiadjra BB, et al. (2011) Fatigue life prediction under variable loading based on a new damage model. *Materials & Design* 32(1): 183–191.
- Aghoury IE and Galal K (2013) A fatigue stress-life damage accumulation model for variable amplitude fatigue loading based on virtual target life. *Engineering Structures* 52: 621–628.
- Ayoub G, Naït-Abdelaziz M, Zaïri F, et al. (2011) A continuum damage model for the high-cycle fatigue life prediction of styrene-butadiene rubber under multiaxial loading. *International Journal of Solids and Structures* 48(18): 2458–2466.
- Böhm E, Kurek M, Junak G, et al. (2014) Accumulation of fatigue damage using memory of the material. *Procedia Materials Science* 3: 2–7.
- Carpinteri A, Spagnoli A and Vantadori S (2003) A multiaxial fatigue criterion for random loading. *Fatigue & Fracture of Engineering Materials & Structures* 26(6): 515–522.
- Chaboche JL and Lesne PM (1998) A non-linear continuous fatigue damage model. *Fatigue & Fracture of Engineering Materials & Structures* 11(1): 1–17.
- Corten HT and Dolan TJ (1956) Cumulative fatigue damage. In: *Proceedings of the international conference on fatigue of metals*, Institution of Mechanical Engineers, ASME, London, pp. 235–246.
- Cui W (2002) A state-of-the-art review on fatigue life prediction methods for metal structures. *Journal of Marine Science and Technology* 7(1): 43–56.
- Cui W, Wang F and Huang X (2011) A unified fatigue life prediction method for marine structures. *Marine Structures* 24(2): 153–181.
- Devulder A, Aubry D and Puel G (2010) Two-time scale fatigue modelling: Application to damage. *Computational Mechanics* 45(6): 637–646.
- Djebli A, Aid A, Bendouba M, et al. (2013) A non-linear energy model of fatigue damage accumulation and its verification for Al-2024 aluminum alloy. *International Journal of Non-Linear Mechanics* 51: 145–151.
- Fang YQ, Hu MM and Luo YL (2006) New continuous fatigue damage model based on whole damage field measurements. *Chinese Journal of Mechanical Strength* 28(4): 582–596.

- Fatemi A and Yang L (1998) Cumulative fatigue damage and life prediction theories: A survey of the state of the art for homogeneous materials. *International Journal of Fatigue* 20(1): 9–34.
- Freudenthal AM and Heller RA (1959) On stress interaction in fatigue and a cumulative damage rule. *Journal of the Aerospace Sciences* 26(7): 431–442.
- Gao H, Huang HZ, Zhu SP, et al. (2014) A modified nonlinear damage accumulation model for fatigue life prediction considering load interaction effects. *The Scientific World Journal*. Article ID 164378, p. 7. Available at: <http://dx.doi.org/10.1155/2014/164378> (accessed 20 January 2014).
- Ghammouri M, Abbadi M, Mendez J, et al. (2011) An approach in plastic strain-controlled cumulative fatigue damage. *International Journal of Fatigue* 33(2): 265–272.
- Huffman PJ and Beckman SP (2013) A non-linear damage accumulation fatigue model for predicting strain life at variable amplitude loadings based on constant amplitude fatigue data. *International Journal of Fatigue* 48: 165–169.
- Kwofie S and Rahbar N (2013) A fatigue driving stress approach to damage and life prediction under variable amplitude loading. *International Journal of Damage Mechanics* 22(3): 393–404.
- Liakat M and Khonsari MM (2014) An experimental approach to estimate damage and remaining life of metals under uniaxial fatigue loading. *Materials & Design* 57: 289–297.
- Lv Z, Huang HZ, Zhu SP, et al. (2015) A modified nonlinear fatigue damage accumulation model. *International Journal of Damage Mechanics* 24(2): 168–181.
- Manson SS and Halford GR (1981) Practical implementation of the double linear damage rule and damage curve approach for treating cumulative fatigue damage. *International Journal of Fracture* 17(2): 169–192.
- McEvily AJ, Ishihara S and Endo M (2005) An analysis of multiple two-step fatigue loading. *International Journal of Fatigue* 27(8): 862–866.
- Miner MA (1945) Cumulative damage in fatigue. *Journal of Applied Mechanics* 12(3): 159–164.
- Morrow JD (1986) The effect of selected sub-cycle sequences in fatigue loading histories. *Random Fatigue Life Predictions*, Vol 72. New York: ASME Publication PVP, pp. 43–60.
- Pavlou DG (2002) A phenomenological fatigue damage accumulation rule based on hardness increasing, for the 2024-T42 aluminum. *Engineering Structures* 24(11): 1363–1368.
- Pereira H, De Jesus AMP, Fernandes AA, et al. (2008) Analysis of fatigue damage under block loading in a low carbon steel. *Strain* 44(6): 429–439.
- Richart FE and Newmark NM (1948) A hypothesis for the determination of cumulative damage in fatigue. *Proceedings of the American Society for Testing and Materials* 48: 767–800.
- Schijve J (2003) Fatigue of structures and materials in the 20th century and the state of the art. *International Journal of Fatigue* 25(8): 679–702.
- Schütz W (1996) A history of fatigue. *Engineering Fracture Mechanics* 54(2): 263–300.
- Shang DG and Yao WX (1999) A nonlinear damage cumulative model for uniaxial fatigue. *International Journal of Fatigue* 21(2): 187–194.
- Shenoy V, Ashcroft IA, Critchlow GW, et al. (2010) Fracture mechanics and damage mechanics based fatigue lifetime prediction of adhesively bonded joints subjected to variable amplitude fatigue. *Engineering Fracture Mechanics* 77(7): 1073–1090.
- Skorupa M (1998) Load interaction effects during fatigue crack growth under variable amplitude loading—A literature review. Part I: Empirical trends. *Fatigue & Fracture of Engineering Materials & Structures* 21(8): 987–1006.
- Skorupa M (1999) Load interaction effects during fatigue crack growth under variable amplitude loading—A literature review. Part II: Qualitative interpretation. *Fatigue & Fracture of Engineering Materials & Structures* 22(10): 905–926.
- Taheri S, Vincent L and Le-roux JC (2013) A new model for fatigue damage accumulation of austenitic stainless steel under variable amplitude loading. *Procedia Engineering* 66: 575–586.
- Tian J, Liu ZM and He R (2012) Non-linear fatigue-cumulative damage model for welded aluminum alloy joint of EMU. *Journal of the China Railway Society* 34(3): 40–43.
- Tikri B, Ngarmaim N, Barka M, et al. (2014) New nonlinear damage law by fatigue based on the curve of Bastenaire. *Global Journal of Researches in Engineering* 14(4): 21–24.

- Van Do VN, Lee CH and Chang KH (2015) High cycle fatigue analysis in presence of residual stresses by using a continuum damage mechanics model. *International Journal of Fatigue* 70: 51–62.
- Xie LY (1995) On the equivalence of fatigue damage states. *Journal of Mechanical Strength* 17(2): 100–104.
- Xie LY, Lv WG and Shi ZF (1994) Experimental study of fatigue damage under two level loading. *Journal of Mechanical Strength* 16(3): 52–54.
- Yang XH, Yao WX and Duan CM (2003) The review of ascertainable fatigue cumulative damage rule. *Engineering Science* 5(4): 82–87.
- Ye DY and Wang ZL (2001) A new approach to low-cycle fatigue damage based on exhaustion of static toughness and dissipation of cyclic plastic strain energy during fatigue. *International Journal of Fatigue* 23(8): 679–687.
- Ye DY, Wang DJ, Tong XY, et al. (1999) A new approach for studying fatigue damage. *Journal of Experimental Mechanics* 14(1): 80–88.
- Yuan R, Li H, Huang HZ, et al. (2015) A nonlinear fatigue damage accumulation model considering strength degradation and its applications to fatigue reliability analysis. *International Journal of Damage Mechanics* 24(5): 646–662.
- Yuan R, Li H, Huang HZ, et al. (2013) A new non-linear continuum damage mechanics model for fatigue life prediction under variable loading. *Mechanika* 19(5): 506–511.
- Yang L and Fatemi A (1998) Cumulative fatigue damage mechanisms and quantifying parameters: A literature review. *Journal of Testing and Evaluation* 26(2): 89–100.
- Zhu SP, Huang HZ and Wang ZL (2011) Fatigue life estimation considering damaging and strengthening of low amplitude loads under different load sequences using Fuzzy sets approach. *International Journal of Damage Mechanics* 20(6): 876–899.
- Zuo FJ, Huang HZ, Zhu SP, et al. (2015) Fatigue life prediction under variable amplitude loading using a non-linear damage accumulation model. *International Journal of Damage Mechanics* 24(5): 767–784.